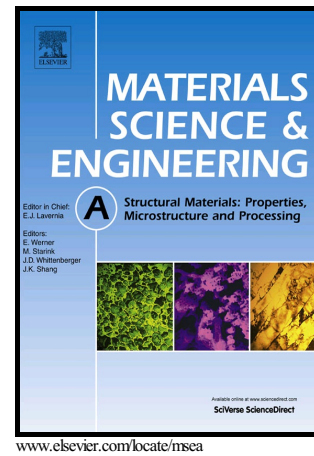


Author's Accepted Manuscript

Macro/microstructure evolution and mechanical properties of Ti33.3Al alloys by adding WC particles

Ruirun Chen, Yingmei Tan, Hongze Fang, Liangshun Luo, Hongsheng Ding, Yanqing Su, Jingjie Guo, Hengzhi Fu



PII: S0921-5093(18)30520-3
DOI: <https://doi.org/10.1016/j.msea.2018.04.025>
Reference: MSA36345

To appear in: *Materials Science & Engineering A*

Received date: 30 November 2017
Revised date: 5 April 2018
Accepted date: 6 April 2018

Cite this article as: Ruirun Chen, Yingmei Tan, Hongze Fang, Liangshun Luo, Hongsheng Ding, Yanqing Su, Jingjie Guo and Hengzhi Fu, Macro/microstructure evolution and mechanical properties of Ti33.3Al alloys by adding WC particles, *Materials Science & Engineering A*, <https://doi.org/10.1016/j.msea.2018.04.025>

This is a PDF file of an unedited manuscript that has been accepted for publication. As a service to our customers we are providing this early version of the manuscript. The manuscript will undergo copyediting, typesetting, and review of the resulting galley proof before it is published in its final citable form. Please note that during the production process errors may be discovered which could affect the content, and all legal disclaimers that apply to the journal pertain.

Macro/microstructure evolution and mechanical properties of Ti33.3Al alloys by adding WC particles

Ruirun Chen^{*}, Yingmei Tan, Hongze Fang, Liangshun Luo, Hongsheng Ding, Yanqing Su, Jingjie Guo, Hengzhi Fu

National Key Laboratory for Precision Hot Processing of Metals, Harbin Institute of Technology, Harbin, 150001, China

Abstract

In order to improve mechanical properties of binary TiAl alloys, Ti33.3Al (weight percent, hereafter in wt.%) alloys with different WC particles content (1.5%, 3.0%, 4.5%, 6.0%, 7.5%) were prepared by vacuum arc melting. The phase constitution, macro/microstructure evolution and mechanical properties were investigated systematically. XRD results showed that WC disappeared and Ti₂AlC phase appeared after adding WC particles because of WC reacting with Ti and Al. In addition, the lattice parameters of α_2 phase increased due to the solid solubility of interstitial carbon atoms and substitutional tungsten atoms. For microstructure, rod-like Ti₂AlC particles formed when WC content was more than 3.0%, and the length diameter ratio of Ti₂AlC particles increased when WC content was 7.5%. It was found that the shape changing of Ti₂AlC was in accordance with the morphology of lamellar colony, which indicated Ti₂AlC firstly formed during solidification. The microstructure changed from coarse columnar to fine equiaxed and the average size of lamellar colony decreased from 189.7 to 66.5 μm with increasing WC content. Tungsten segregated and formed a little B2 phase in the lamellar colony when the WC

content was more than 6.0%. Compressive testing showed that the strength and the strain were improved from 1847 to 2324 MPa and from 25.7 to 28.5%, respectively. The Vickers hardness of Ti33.3Al alloys was also improved by the addition of WC. The improvement of mechanical properties was caused by the grain refinement, solid solution of carbon and tungsten atoms, reinforcement of Ti_2AlC phase and a little B2 phase.

Keywords: TiAl; WC; Ti_2AlC ; Microstructure; Mechanical properties

1. Introduction

TiAl alloys are considered to be promising materials and are widely used in aerospace, marine and automobile industry instead of nickel based superalloys [1, 2]. In spite of many excellent properties such as excellent corrosion resistance, low density, good creep properties [3, 4], TiAl alloys have poor ductility at room temperature, which hinders the further application [5].

In-situ formed reinforcements have attracted much attention due to the advantage of compatible interfaces with matrix [6]. As TiB_2 [7], Ti_2AlC [8], Ti_2AlN [9], Y_2O_3 [10] and Al_2O_3 [11] are proved to be suitable reinforcements to enhance the mechanical properties of TiAl alloys, interstitial elements such as C, N, B are selected for the preparation of composite materials. The $Ti_2AlC/TiAl$ composites with different (Nb–C) content were fabricated by Shu et al. using combustion synthesis method and the best compression property was obtained with 10 wt.% (Nb–C) elements [12]. Compared with the nominal $Ti_{43.5}Al_{14}Nb_1Mo_{0.1}B$ alloy, the α_2/γ lamellar colony microstructure in TiAl alloys was refined with carbon atoms addition and the microhardness was improved [13].

In recent years, W, Cr, V, and Nb have been added into the TiAl alloys to optimize the microstructure and improve the mechanical properties [14-16]. W as a strong β phase stabilizer was known to increase creep resistance and tensile properties of TiAl alloys, which could retard dislocation motion and stabilize lamellae microstructure [17-19]. In addition, Hu et al. [20] have found that W could improve the ductility of TiAl alloys using first-principles study.

Due to the good effect of Mn on the ductility [21], Shu et al. [22] have added Mn into the $Ti_2AlC/TiAl$ composites and the results showed that the strength and ductility of TiAl alloys could be enhanced synchronously. From the above analysis, it can be seen that the combination of alloying and composites in TiAl alloys shows better effect on the mechanical properties. On account of the good effects of W atoms such as improving the ductility of TiAl alloys [20] and the advantages of Ti_2AlC reinforcements such as low density, superior thermal shock resistance, suitable thermal expansion coefficient [23, 24], it can be predicated that TiAl alloys will exhibit refined microstructure and excellent mechanical properties with the combination of C and W. In the present work, C and W are added into Ti33.3Al alloys simultaneously in the form of WC particles, and the effect of WC addition on the mechanical properties of Ti33.3Al alloys will be discussed systematically.

2. Experimental methods

The Ti33.3Al (weight percent, hereafter in wt.%) alloy button ingots with increasing WC content (1.5, 3.0, 4.5, 6.0, 7.5%) were prepared by vacuum arc furnace under the protection of argon atmosphere. Raw materials were sponge titanium (99.98% purity), aluminum (99.98%) and WC particles (99.9%). The samples were re-melted for four times to homogenize the chemical composition. The phase constitution was analyzed by X-ray diffraction (XRD) with Cu $K\alpha$ radiation. Macrostructure was

photographed by Nikon Digital Single Lens Reflex. Microstructure was analyzed by Optical Microscope (OM) and Quanta 200F scanning electron microscopy (SEM) equipped with Energy Dispersive Spectrometer (EDS). The specimens for macro/microstructure observation were cut vertically from the center of the button and were etched by solution of hydrofluoric acid, nitric acid and water (HF: HNO₃: H₂O is 1: 3: 16, volume fraction) for 15s. Cylindrical specimens with a size of $\varnothing 4 \times 6$ mm were used for compressive test. And the compressive tests were conducted on Instron 5569 electronic testing machine with the loading rate of 0.5 mm/min. Microhardness measurements were operated on digital microhardness tester under load of 200g for 15s. To ensure the accuracy of the data, at least three specimens of each composition sample were tested for compressive properties, and the microhardness was measured at ten different positions of each sample, the average values were calculated based on these data.

3. Results and Discussion

3.1. Effects of WC on the phase constitution of Ti33.3Al alloys

The X-ray diffraction patterns are displayed in Fig. 1(a). Ti33.3Al alloy and Ti33.3Al alloy with 1.5% WC mainly consist of γ -TiAl and α_2 -Ti₃Al phase. As the addition of WC is 3.0, 4.5, 6.0 and 7.5% respectively, the strongest peak of Ti₂AlC appears at the diffraction angle of 39.84°. And the diffraction peak of WC is not observed, which indicates that there is reaction among Ti, Al and WC during the solidification process. The strongest diffraction peak of α_2 phase is locally amplified as displayed in Fig. 1(b). And the diffraction angle of the α_2 peak is gradually shifted to the left with increasing WC content.

Fig. 1(b) shows that $\sin\theta$ decreases while interplanar spacing increases, which indicates that the lattice distortion of α_2 phase occurs. It has been reported that carbon

as interstitial atoms tends to dissolve in α_2 phase due to the presence of T_6 type sites in the α_2 phase [25]. In addition, tungsten as substitutional atoms can result in the increased lattice of α_2 phase. Both of them contribute to the lattice distortion of α_2 phase.

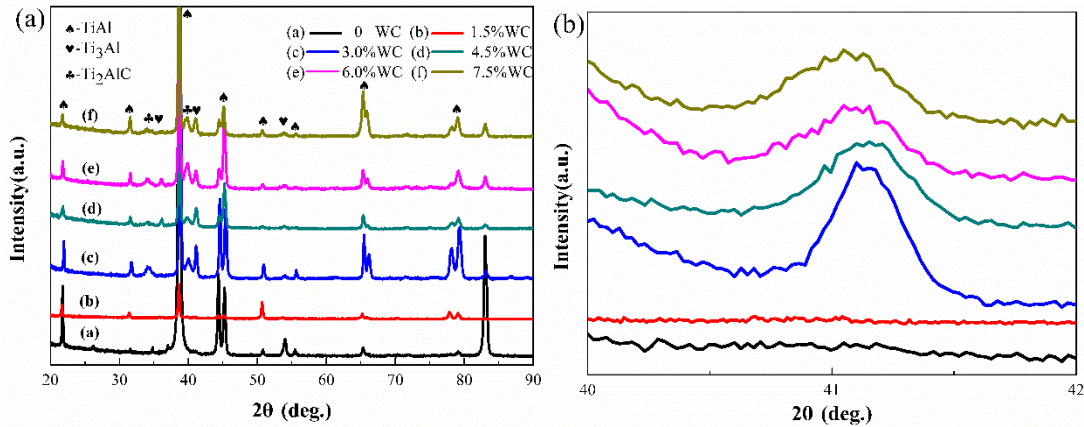


Fig. 1. (a) XRD patterns of Ti33.3Al alloy with different WC content; (b) magnification of α_2 peak

3.2. Macrostructure of Ti33.3Al alloys with increasing WC content

Fig. 2 shows the macrostructure evolution of Ti33.3Al alloys with increasing WC content. Without WC, the macrostructure of the Ti33.3Al alloy presents a typical coarse-grained columnar macrostructure. When the content of WC is 1.5%, the macrostructure changes to large dendrites grains significantly. The grain size is further reduced and tends to be uniform with increasing WC content.

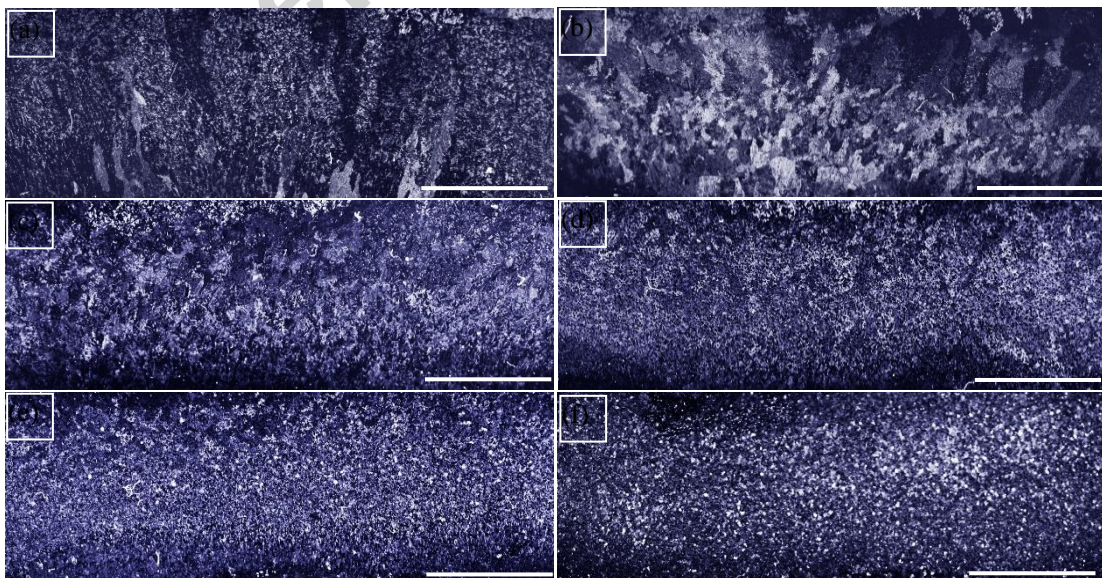


Fig.2. Macrostructure of Ti33.3Al alloys with increasing WC content (a) 0; (b) 1.5%; (c) 3.0%; (d) 4.5%; (e) 6.0%; (f) 7.5%

3.3. Microstructure of Ti33.3Al alloys with increasing WC content

Fig.3 displays the microstructure evolution of Ti33.3Al alloys with increasing WC content. The microstructure of Ti33.3Al alloy without WC shows coarse columnar dendrites. When the addition of WC is 1.5%, the coarse columnar grains change to fine dendrites and a number of large γ phases exist in the dendritic gap. The coarse lamellar colony is further reduced with 3.0% WC, and a few Ti_2AlC particles form in the α_2/γ lamellar colony. When the content of WC reaches 4.5, 6.0 and 7.5%, the thick dendrites gradually transform into fine equiaxed grains and rod-like Ti_2AlC particles distribute more uniformly in the α_2/γ lamellae. It is observed that the length diameter ratio of Ti_2AlC particles in Ti33.3Al alloys increases with 7.5% WC content, which results in increasing size of α_2/γ lamellar colony. The large size of dendrites results in a large interdendritic region, which forms the large γ phase. With the increasing WC content, the smaller size and equiaxed grains decrease the interdendritic region, which contributes to the formation of smaller γ phases. Therefore, accompanied with the refined α_2/γ lamellae, the size of γ phases is gradually reduced. As a result, the Ti33.3Al alloys with increasing WC content show more refined duplex microstructure.

Fig.4 shows the SEM microstructure of Ti33.3Al alloys with increasing WC content. Chen et al. [26] have reported that β -solidification and α -solidification are two modes of solidification in TiAl alloys. Compared with the microstructure of Ti33.3Al alloy, the angle between the primary and secondary dendritic arm changes from 90° to 60° with increasing WC content, which indicates that the addition of WC changes the primary phase of Ti33.3Al alloy from β to α phase. Previous studies reported that N could make the Al elements enriched in solid-liquid interface by

suppressing the diffusion of Al [9]. Therefore, a high N content leads to a shift of the higher Al content solidification pathway, which promotes the formation of α phase. As the C is an α -stabilizer element [13], it can expand the α phase region and change the solidification pathway. Similarly, we can infer that the effect of C during the non-equilibrium solidification process could also promote the formation of α phase. Therefore, the actual solidification path of Ti33.3Al alloy with increasing WC content reduces component segregation by avoiding the peritectic reaction, and α phase becomes the primary phase.

Wang et al. [27] have reported that the TiB precipitates provide nucleation sites for α phase and alter the corresponding morphologies. Similarly, it can be observed that the morphology of α_2/γ lamellar colony is consistent with the change trend of the reinforcements morphology (marked in Fig. 4(f)), which illustrates that the Ti_2AlC particles act as nucleation sites and alter the corresponding morphologies of α_2/γ lamellae. Ti_2AlC particles are prior to precipitating at high temperature before the solid-state phase transformations, and the forming temperature of Ti_2AlC particles is in the range of $\beta + \alpha$ phase [28]. In addition, J. Lapin et al. reported that the spherical and irregular shaped Ti_2AlC particles were formed by transformation of TiC_{1-x} particles, and the formation of plate-like Ti_2AlC particles was in the $L + Ti_2AlC$ phase region [29]. According to the shapes of Ti_2AlC particles in our work, we can confirm that Ti_2AlC particles are formed directly from the melt. Therefore, Ti_2AlC particles are considered to act as nucleation sites during the solidification process, and the α_2/γ lamellae adhere to the Ti_2AlC particles to grow up. W as strong β stabilizing element can result in the residual β phase in the form of B2-structure [30]. As shown in Fig.4 (e) and (f), streamlined tungsten segregation exists in the α_2/γ lamellae and forms a little B2 phase with 6.0% and 7.5% WC content, which indicates that the content of

tungsten atoms exceeds the limit of solid solubility in lamellae. From above analysis, the solidification path of Ti33.3Al alloy can be concluded as follows:

$L \rightarrow L + \beta \rightarrow L + \beta + \alpha \rightarrow \alpha \rightarrow \alpha + \gamma \rightarrow \alpha_2/\gamma + \gamma$. When the WC content is 6.0%, the

solidification path can be concluded as follows:

$L \rightarrow L + \alpha + \beta + Ti_2AlC \rightarrow \alpha + \beta_r + Ti_2AlC \rightarrow \alpha + \gamma + \beta_r + Ti_2AlC \rightarrow \alpha_2/\gamma + \gamma + B2 + Ti_2AlC$.

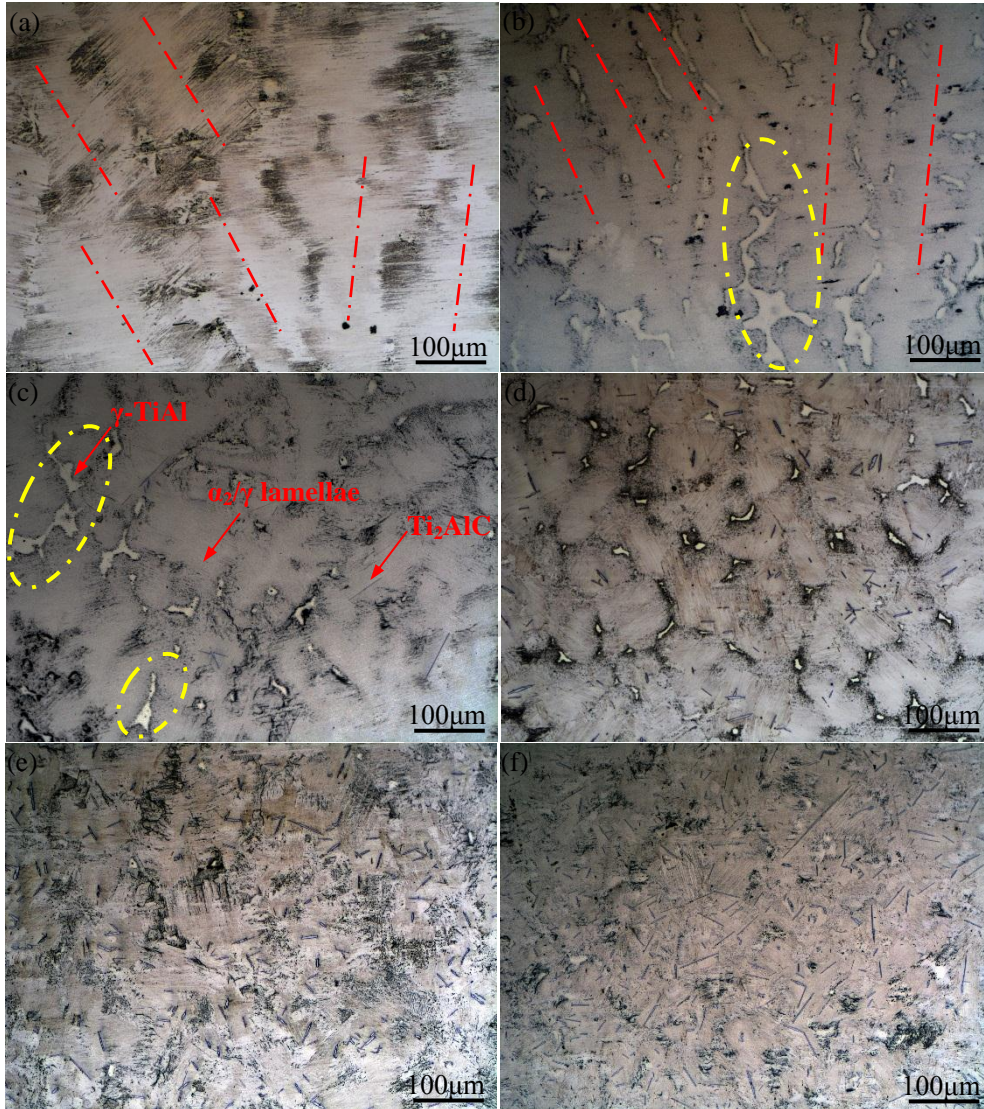


Fig.3. OM microstructure of Ti33.3Al alloys with different WC content (a) 0; (b) 1.5%; (c) 3.0%; (d) 4.5%; (e) 6.0%; (f) 7.5%

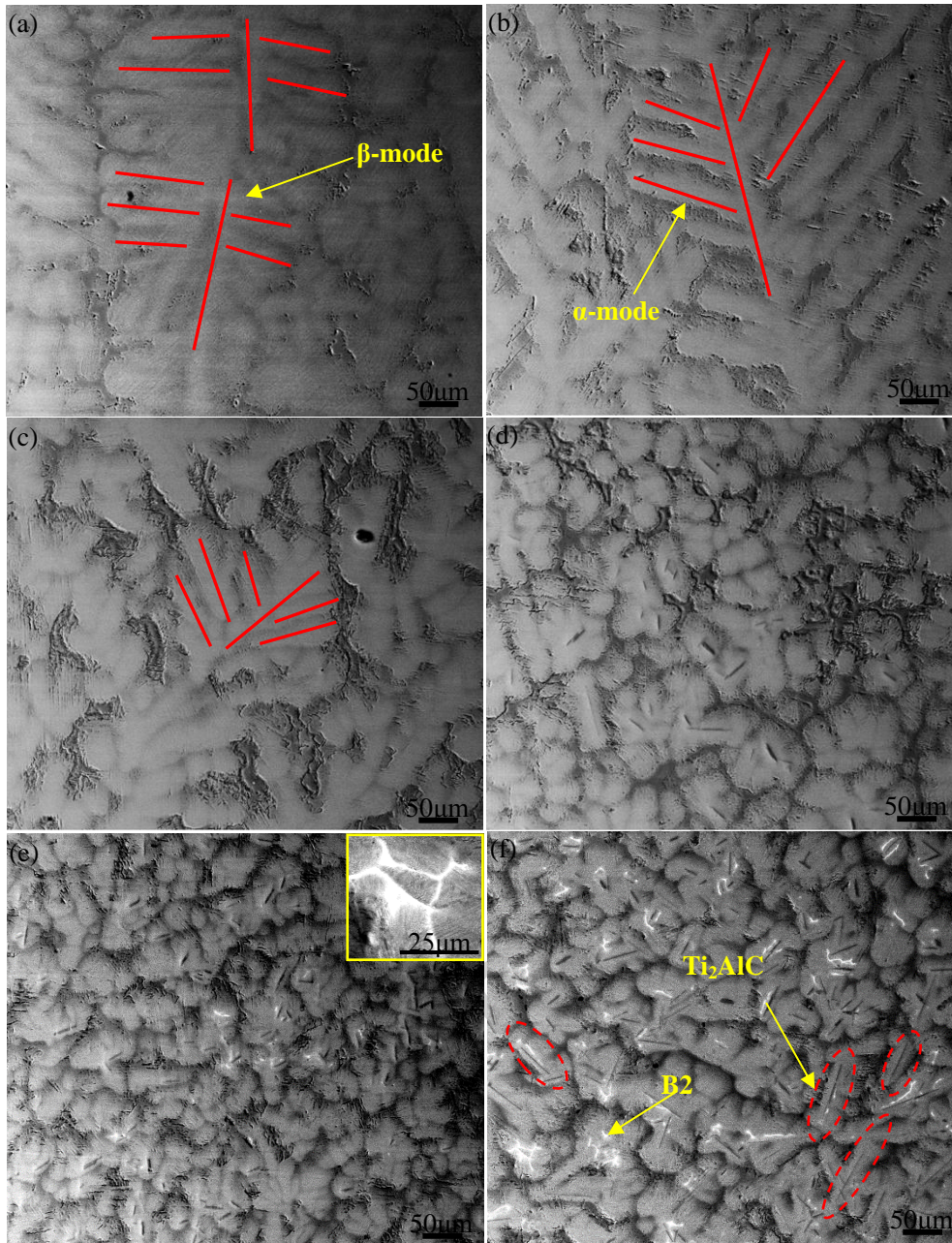


Fig.4. SEM microstructure of Ti33.3Al alloys with increasing WC content (a) 0; (b) 1.5%; (c) 3.0%; (d) 4.5%; (e) 6.0%; (f) 7.5%

As shown in Fig. 5, the specific effect of WC addition on the lamellar colony of Ti33.3Al alloy is illustrated. The primary dendritic arm spacing is used to represent the lamellar colony size for Ti33.3Al alloy and Ti33.3Al alloy with 1.5% WC. According to the scaleplate, the primary dendritic arm spacing was obtained by measuring the distance between the parallel lines in the OM images, which is marked as red line shown in Fig. 3(a) and (b). With higher WC content, average size of

lamellar colony is measured by intersection linear method [31]. And at least five micrographs have been adopted to determine the average size of lamellar colony. Therefore, the size of lamellar colony is 189.7 ± 68.78 , 132.5 ± 43.7 , 124.3 ± 36 , 87.4 ± 20.5 , 66.5 ± 13.9 and 77.6 ± 25.6 μm , respectively.

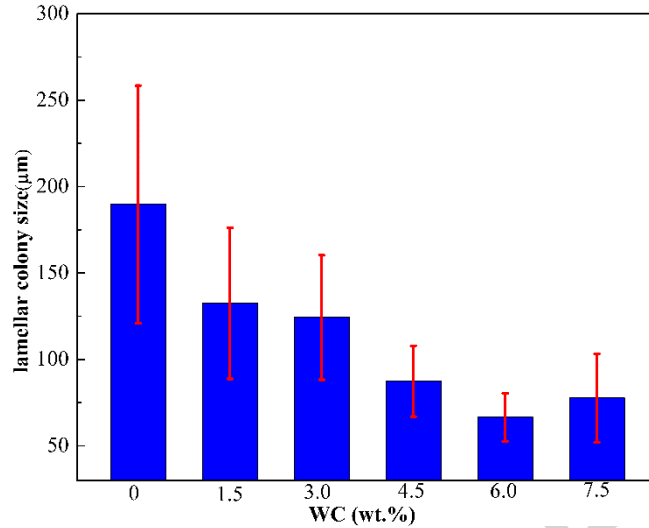


Fig.5. Effect of WC content on the lamellar colony size of Ti33.3Al alloy

Fig. 6 indicates that carbon atoms show inhomogeneous distribution in the Ti33.3Al alloy with 1.5% WC content. A number of carbon atoms gather up at the boundary of α_2/γ lamellae and γ -TiAl phase, which implies the carbon atoms move from the γ phase to the grain boundary due to the lower solid solubility in γ phase [25, 32]. Previous study reported that carbon atoms played a role in blocking the boundary of α_2/γ lamellae and γ phase [33]. The carbon atoms at the grain boundaries can also act as pinning dislocation to increase the strength of alloys.

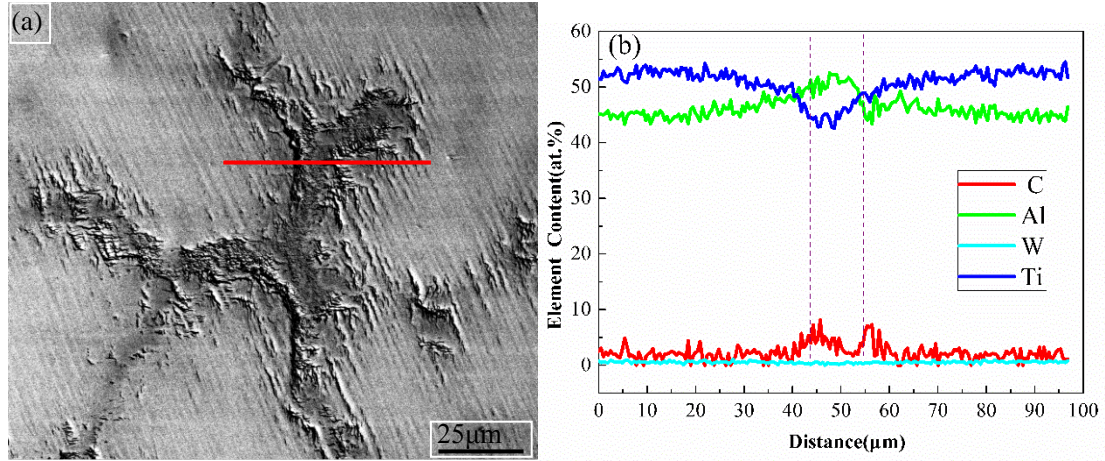
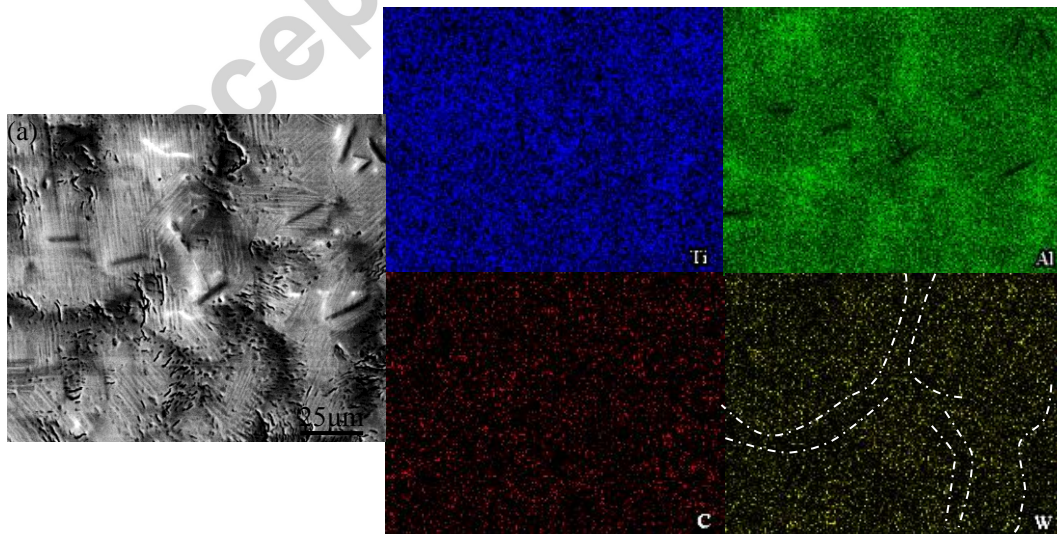


Fig.6. EDS results of Ti33.3Al alloy with 1.5% WC content

Element surface scanning analysis is conducted and the specific distribution of elements in Ti33.3Al alloy is shown in Fig. 7. Fig. 7(a) shows that titanium as the main element distributes uniformly in Ti33.3Al alloy. While aluminum shows obvious segregation in the interdendritic region, which is named of typical S-type segregation. Tungsten as β stabilizer tends to distribute in the α_2/γ lamellae and is absent in the interdendritic region, which is in accord with the report that V, Cr, Mo, Ta, and W are prone to dissolve in α_2 phase [34]. As shown in Fig. 7(b), reinforcements are depleted in aluminum and contain higher titanium and carbon, which is consistent with the result of XRD analysis.



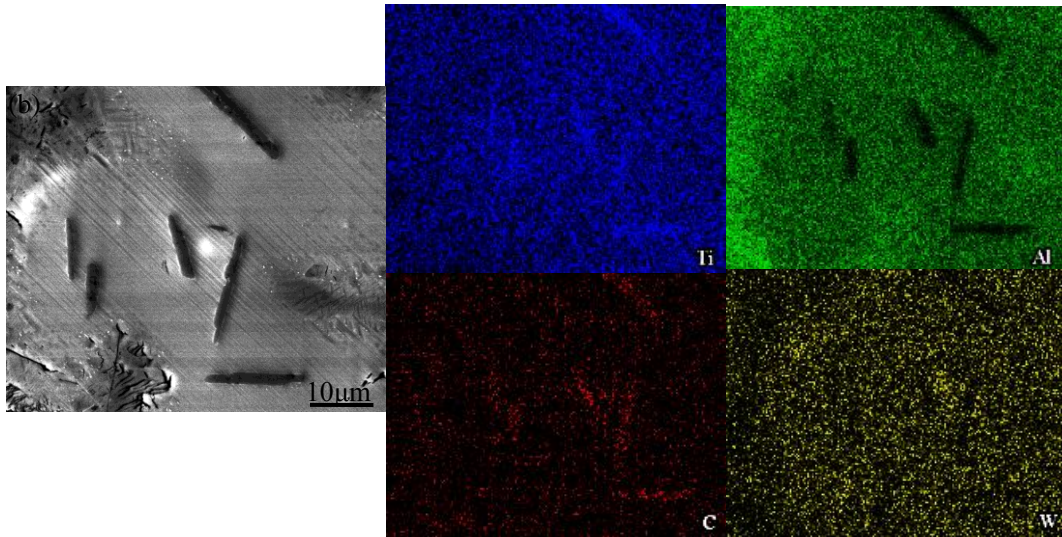


Fig.7. Composition distribution of Ti33.3Al alloys with WC content (a) 6.0% WC; (b) 7.5% WC

Schematic diagram is used to compare the different microstructures in Ti33.3Al alloy with 1.5% and 7.5% WC content. As shown in Fig. 8(a), carbon atoms preferentially exist at the boundary and tungsten atoms mainly dissolve in the α_2/γ lamellae by solid solution. Apart from the solid solution of C atoms, Fig. 8(b) shows that Ti_2AlC particles form with 7.5% WC content and distribute in the lamellae. Tungsten atoms as β stabilizers mainly exist in the B2 phase.

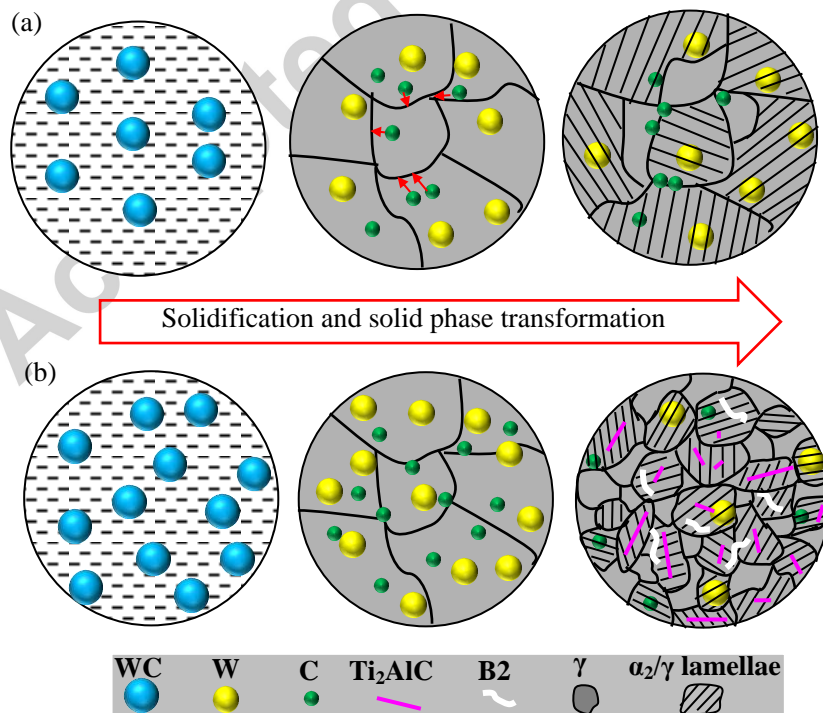


Fig.8. Schematic diagram of Ti33.3Al alloys with WC content (a) 1.5% WC; (b) 7.5% WC

3.4. Mechanical performances of the Ti33.3Al alloy with increasing WC content

In order to investigate the effect of WC on the mechanical properties of the Ti33.3Al alloy, compressive properties are tested at room temperature. As shown in Table 1 and Fig. 9, the compressive strength and strain with increasing WC content show a similar changing trend.

Compared with the mechanical properties of the Ti33.3Al alloy, the compressive strength and strain change slightly when the WC content is 1.5% and 3.0%. Chen et al. [26] have reported that the β -solidification mode is better for axial mechanical properties due to the small angle between lamella and axial direction. When the addition of WC is 1.5% and 3.0%, the solidification mode of Ti33.3Al alloy changes from β to α mode, and the size of lamellar colony decreases slightly. The two factors can explain the slight changes of mechanical properties with 1.5% and 3.0% WC content.

When the content of WC is 4.5% and 6.0%, both of the compressive strength and strain increase and reach a maximum value with 6.0% WC content. Best enhancement on compressive strength and strain are 2324 MPa and 28.5%, respectively. The strengthening mechanism can be concluded from the following aspects. Ti_2AlC acts as nucleation site during the solidification process. It can increase the nucleation rate of α phase and result in the refined α_2/γ lamellae. The Ti33.3Al alloys with increasing WC content show more refined duplex microstructure. Grain refinement increases the number of grain boundaries, which is beneficial to the mechanical properties by impeding the movement of dislocations. Load transfer strengthening of Ti_2AlC reinforcement also contributes to the improvement of mechanical properties. The elastic modulus of Ti_2AlC (278 GPa) [35] is higher than that of TiAl alloy (160-175

GPa) [36]. Previous study has shown that the stress would transfer from the matrix with lower stiffness to reinforcements with higher stiffness in composite materials [37]. Ti_2AlC was coherent with the TiAl matrix fabricated by vacuum arc-melting [38]. Therefore, Ti_2AlC particles could improve the compressive strength effectively by undertaking more transferred load during the stress process. Another important strengthening mechanism is solid solution strengthening. The partition coefficient of W is $K_W^{s/l} = 1.3$ and W has low diffusion coefficient [30]. The refined grains increase the contact area between the solid phase and liquid, which reduces the distance of Tungsten element diffusion and obtains minimum segregation of W. Tungsten atoms in the matrix cause solid solution effect and also stabilize the α_2/γ lamellae [20], which can contribute to the enhancement of strength. Carbon as interstitial atoms cause the lattice distortion. The atoms gather around the dislocations to form the Cottrell atmosphere, which can increase the strength by impeding the dislocation movement.

When the content of WC is 7.5%, the compressive strength and strain decline. It has been reported that borides with short bars or blocks shape are good for the mechanical properties while long curved ribbons as crack sources can deteriorate it [39]. Fig. 4(f) shows that the length diameter ratio of the Ti_2AlC increases with 7.5% WC content and is followed by the increasing size of α_2/γ lamellae, which can account for the decline of compressive properties. Similar to the negative effect of too much solid solution of Mn on the ductility of the $\text{Ti}_2\text{AlC}/\text{TiAl}$ composites [22], the severe lattice distortion resulting from too much solid solution of W in the composites leads to the split of TiAl matrix, which is detrimental to the compressive strain of the Ti33.3Al alloy with 7.5% WC content. A higher volume fraction of B2 phase exists in the matrix of Ti33.3Al alloy with 7.5% WC content. Wang et al. reported that B2

phase was a source of cracks due to its brittleness in the compression test at room temperature [40]. Previous study showed that the deformation incompatibilities caused the concentration of stress at the interface of B2 phase and the matrix, which resulted in the cracks [41]. All of these can explain the decreased compressive strength and strain in the compression test.

Table 1 Compressive properties of the Ti33.3Al alloy with different WC

Content	Compressive Strength (MPa)	Compressive Strain (%)
0	1847±45	25.7±0.68
1.5	1913±23	25.6±1.15
3.0	1917±37	25.4±0.75
4.5	2189±20	27.8±0.59
6.0	2324±22	28.5±0.28
7.5	2112±23	24.8±1.02

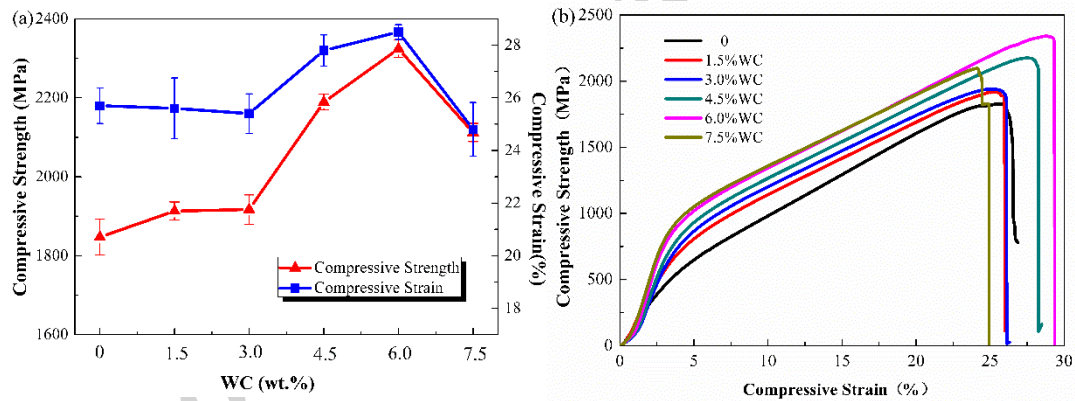


Fig.9. Compressive properties of Ti33.3Al alloy with increasing WC content (a) compressive strength and compressive strain; (b) compressive strain-stress curve

Fig.10 shows that the Vickers hardness value is improved from 352 to 450 HV with increasing WC content. The main reasons for the improvement of Vickers hardness can be concluded as follows: It has been reported that the hardness of Ti_2AlC and TiAl alloy is 4.9 and 3.15 GPa, respectively [38], which indicates that the hardness of Ti_2AlC is higher than that of TiAl alloy. Therefore, the presence of

Ti₂AlC particles can lead to the improvement of Vickers hardness. In addition, the higher Vickers hardness results from the reduced size of γ phase, as γ -TiAl phase is the softest among the B2, α_2 and γ phase [42]. Solid solution strengthening and volume fraction of B2 phase are all beneficial for the Vickers hardness of TiAl composites.

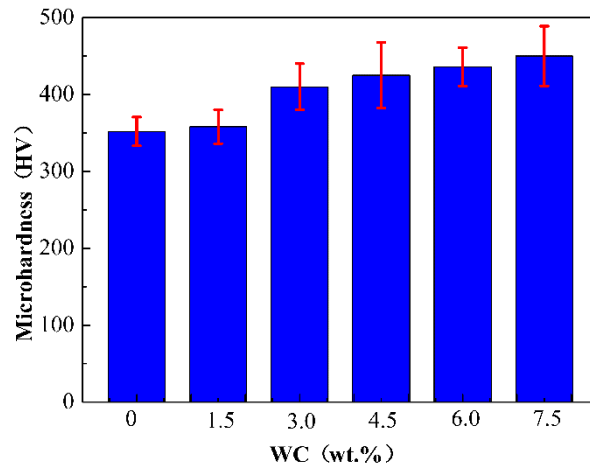


Fig.10. Microhardness of Ti33.3Al alloys with increasing WC content

3.5. Fracture surface analysis of Ti33.3Al alloy with different WC addition

Fig. 11 shows the fracture section near big fracture surface. It can be seen that carbide plays an effective role in impeding crack propagation. Reinforcements can change and terminate the crack propagation path by tearing, bridging ligament and decohesion, which reduces the break energy to relieve the inherent brittle fracture. All of the microstructures mean that the reinforcements contribute to the improvement of mechanical properties.

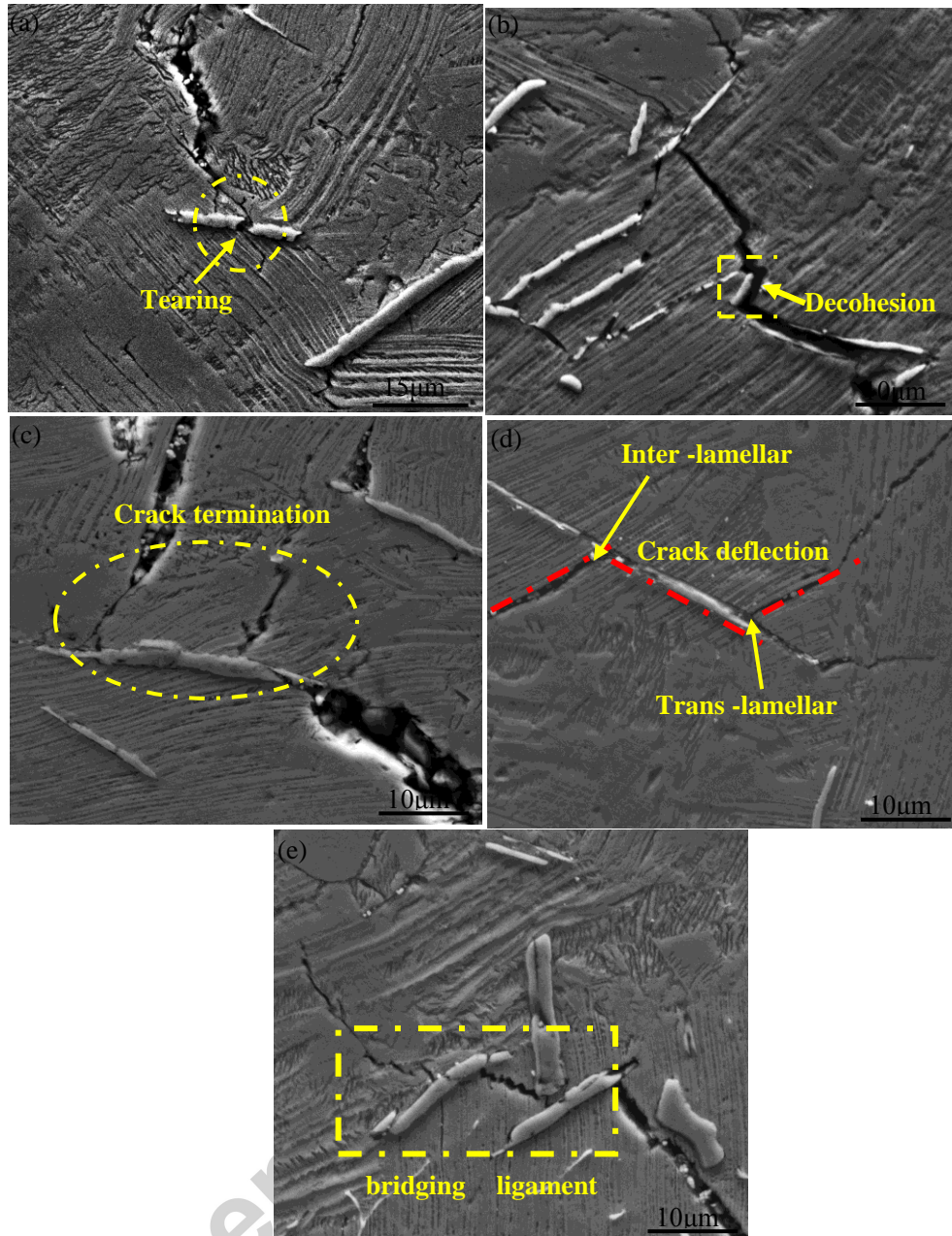


Fig.11. Microstructure of longitudinal sections near the fracture surface

Big flat facets and rapid expansion of the main crack can be observed without WC addition in Fig. 12(a), which indicates the poor fracture mechanism of Ti33.3Al at room temperature. Interlamellar fracture and translamellar fracture are found in the Ti33.3Al alloy with 1.5% WC, which also exhibits the brittle cleavage fracture. Compared with Fig. 12(a) and (b), the fracture of α_2/γ lamella is refined with the increased addition of WC, which results from the refined grains and implies the

improvement of mechanical properties. From the magnified image, there is extraction of reinforcement in the fracture surface.

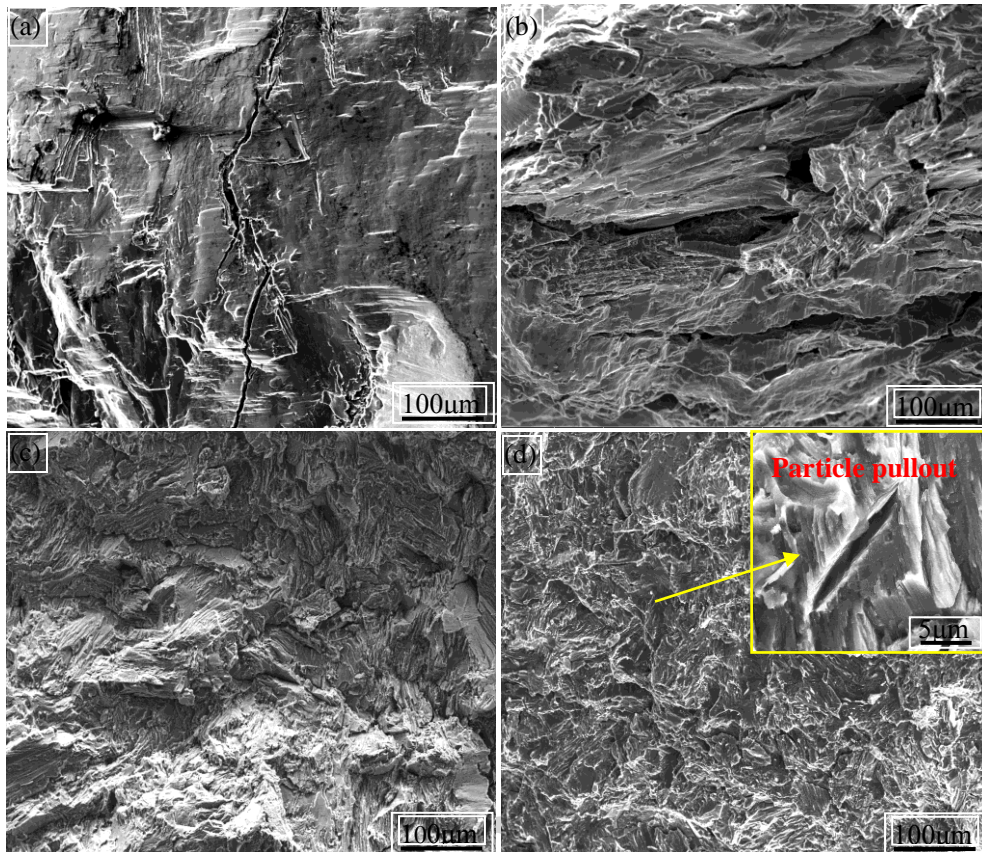


Fig. 12. Fracture morphology of Ti33.3Al alloys with increasing WC content (a) 0; (b) 1.5% ; (c) 6.0%; (d) 7.5%

Conclusions

In this paper, the macro/microstructure evolution and mechanical properties in Ti33.3Al with different content of WC were investigated. The following conclusions can be drawn:

- (1) Ti_2AlC phase forms when WC content is more than 3.0%. The shape of Ti_2AlC phase changes from rod-like to needle-like with increasing WC content. The changing shape of Ti_2AlC phase is in accordance with the morphology of α_2/γ lamellar colony.

- (2) Ti_2AlC phase acts as heterogenous nucleation sites during solidification. The microstructure of $\text{Ti}_{33.3}\text{Al}$ alloys is refined obviously, and the coarse columnar grains transform into fine equiaxed grains with increasing WC content.
- (3) The $\text{Ti}_{33.3}\text{Al}$ alloy with 6.0% WC exhibits the best compressive properties with the strength and the strain of 2324 MPa and 28.5% respectively. The microhardness increases continuously with increasing WC content. The strengthening mechanisms are the grain refinement, solid solution of carbon and tungsten atoms, reinforcement of Ti_2AlC phase and a little B2 phase.
- (4) Carbide impedes crack propagation and reduces the break energy by tearing, decohesion and bridging ligament, which contributes to the improvement of mechanical properties.

Acknowledgements

This work was supported by National key research and development program of China (2017YFA0403802) and National Natural Science Foundation of China (51741404 and 51331005).

References

- [1] M. Yamaguchi, H. Inui, K. Ito, High-temperature structural intermetallics, *Acta Mater.* 48 (2000) 307-322.
- [2] J. Cheng, F. Li, S. Zhu, Y. Yu, Z. Qiao, J. Yang, Electrochemical corrosion and tribological evaluation of TiAl alloy for marine application, *Tribology International* 115 (2017) 483-492.
- [3] H. Clemens, S. Mayer, Design, Processing, Microstructure, Properties, and Applications of Advanced Intermetallic TiAl Alloys, *Adv. Eng. Mater.* 15 (2013) 191-215.
- [4] F. Appel, H. Clemens, F.D. Fischer, Modeling concepts for intermetallic titanium aluminides, *Prog. Mater. Sci.* 81 (2016) 55-124.
- [5] J. Lapin, A. Klimová, Z. Gabalcová, T. Pelachová, O. Bajana, M. Štamborská, Microstructure and mechanical properties of cast in-situ TiAl matrix composites reinforced with $(\text{Ti,Nb})_2\text{AlC}$ particles, *Mater. Design* 133 (2017) 404-415.

- [6] Y. Jiao, L.J. Huang, Q. An, S. Jiang, Y.N. Gao, X.P. Cui, L. Geng, Effects of Ti 5 Si 3 characteristics adjustment on microstructure and tensile properties of in-situ (Ti 5 Si 3 +TiBw)/Ti6Al4V composites with two-scale network architecture, *Mat. Sci. Eng. A* 673 (2016) 595-605.
- [7] Z.W. Huang, W. Hu, Thermal stability of an intermediate strength fully lamellar Ti-45Al-2Mn-2Nb-0.8 vol.% TiB₂ alloy, *Intermetallics* 54 (2014) 49-55.
- [8] H.F. Sun, X.W. Li, P. Zhang, W.B. Fang, The microstructure and tensile properties of the Ti₂AlC reinforced TiAl composites fabricated by powder metallurgy, *Mat. Sci. Eng. A* 611 (2014) 257-262.
- [9] T. Zhang, Z. Wu, R. Hu, F. Zhang, H. Kou, J. Li, Influence of nitrogen on the microstructure and solidification behavior of high Nb containing TiAl alloys, *Mater. Design* 103 (2016) 100-105.
- [10] H. Ding, H. Zhang, Q. Wang, R. Chen, J. Guo, H. Fu, Effect of Y₂O₃ particles on the fracture toughness of directionally solidified TiAl-based alloys, *Mat. Sci. Eng. A* 703 (2017) 108-115.
- [11] L. Xiang, F. Wang, J. Zhu, X. Wang, Mechanical properties and microstructure of Al₂O₃/TiAl in situ composites doped with Cr₂O₃, *Mat. Sci. Eng. A* 528 (2011) 3337-3341.
- [12] S. Shu, F. Qiu, S. Jin, J. Lu, Q. Jiang, Compression properties and work-hardening behavior of Ti₂AlC/TiAl composites fabricated by combustion synthesis and hot press consolidation in the Ti-Al-Nb-C system, *Mater. Design* 32 (2011) 5061-5065.
- [13] E. Schwaighofer, B. Rashkova, H. Clemens, A. Stark, S. Mayer, Effect of carbon addition on solidification behavior, phase evolution and creep properties of an intermetallic β -stabilized γ -TiAl based alloy, *Intermetallics* 46 (2014) 173-184.
- [14] I. Gil, M.A. Munoz-Morris, D.G. Morris, The effect of heat treatments on the microstructural stability of the intermetallic Ti-46.5Al-2W-0.5Si, *Intermetallics* 9 (2001) 373-385.
- [15] J.G. Wang, T.G. Nieh, Creep of a beta phase-containing TiAl alloy, *Intermetallics* 8 (2000) 737-748.
- [16] A.V. Kartavykh, E.A. Asnis, N.V. Piskun, I.I. Statkevich, M.V. Gorshenkov, A.V. Korotitskiy, Room-temperature tensile properties of float-zone processed β -stabilized γ -TiAl(Nb,Cr,Zr) intermetallic, *Mater. Lett.* 188 (2017) 88-91.
- [17] W.R. Chen, J. Beddoes, L. Zhao, Effect of aging on the tensile and creep behavior of a fully lamellar near γ -TiAl alloy, *Mat. Sci. Eng. A* 323 (2002) 306-317.
- [18] H.L. Sun, Z.W. Huang, D.G. Zhu, X.S. Jiang, Dendrite core grain refining and interdendritic coarsening behaviour in W-containing γ -TiAl based alloys, *J. Alloy Compd.* 552 (2013) 213-218.
- [19] R. Yu, L.L. He, Z.Y. Cheng, J. Zhu, H.Q. Ye, B₂ precipitates and distribution of W in a Ti-47Al-2W-0.5Si alloy, *Intermetallics* 10 (2002) 661-665.
- [20] H. Hu, X. Wu, R. Wang, W. Li, Q. Liu, Phase stability, mechanical properties and electronic structure of TiAl alloying with W, Mo, Sc and Yb: First-principles study, *J. Alloy Compd.* 658 (2016) 689-696.
- [21] T.K. Lee, E.I. Mosunov, S.K. Hwang, Consolidation of a gamma TiAl-Mn-Mo alloy by elemental powder metallurgy, *Mat. Sci. Eng. A* 239-240 (1997) 540-545.
- [22] S.L. Shu, F. Qiu, B. Xing, S.B. Jin, Y.W. Wang, Q.C. Jiang, Study of effect of Mn addition on the mechanical properties of Ti₂AlC/TiAl composites through

- first principles study and experimental investigation, *Intermetallics* 28 (2012) 65-70.
- [23] J. Zhu, N. Han, A. Wang, Synthesis, microstructure and mechanical properties of $(\text{Ti}_{1-x}\text{Nb}_x)_2\text{AlC}/\text{Al}_2\text{O}_3$ solid solution composites, *Mat. Sci. Eng. A* 558 (2012) 7-12.
- [24] T. Ai, N. Yu, X. Feng, N. Xie, W. Li, P. Xia, Low-temperature synthesis and characterization of $\text{Ti}_2\text{AlC}/\text{TiAl}$ in situ composites via a reaction Hot-Pressing Process in the Ti_3AlC_2 -Ti-Al system, *Metals and Materials International* 21 (2015) 179-184.
- [25] A. Menand, A. Huguet, A. NeracPartaix, Interstitial solubility in gamma and alpha(2) phases of TiAl-based alloys, *Acta Mater.* 44 (1996) 4729-4737.
- [26] R. Chen, S. Dong, J. Guo, H. Ding, Y. Su, H. Fu, Investigation of macro/microstructure evolution and mechanical properties of directionally solidified high-Nb TiAl-based alloy, *Mater. Design* 89 (2016) 492-506.
- [27] J. Wang, X. Guo, J. Qin, D. Zhang, W. Lu, Microstructure and mechanical properties of investment casted titanium matrix composites with B_4C additions, *Mat. Sci. Eng. A* 628 (2015) 366-373.
- [28] Z. Wu, R. Hu, T. Zhang, F. Zhang, H. Kou, J. Li, Understanding the role of carbon atoms on microstructure and phase transformation of high Nb containing TiAl alloys, *Materials Characterization* 124 (2017) 1-7.
- [29] J. Lapin, M. Štamborská, T. Pelachová, O. Bajana, Fracture behaviour of cast in-situ TiAl matrix composite reinforced with carbide particles, *Mat. Sci. Eng. A* 721 (2018) 1-7.
- [30] D. Daloz, U. Hecht, J. Zollinger, H. Combeau, A. Hazotte, M. Založnik, Microsegregation, macrosegregation and related phase transformations in TiAl alloys, *Intermetallics* 19 (2011) 749-756.
- [31] Y. Liu, R. Hu, J. Yang, J. Li, Tensile properties and fracture behavior of in-situ synthesized $\text{Ti}_2\text{AlN}/\text{Ti}_{48}\text{Al}_{12}\text{Cr}_2\text{Nb}$ composites at room and elevated temperatures, *Mat. Sci. Eng. A* 679 (2017) 7-13.
- [32] Q. Wang, H.S. Ding, H.L. Zhang, R.R. Chen, J.J. Guo, H.Z. Fu, Variations of microstructure and tensile property of gamma-TiAl alloys with 0-0.5 at% C additives, *Mat. Sci. Eng. A* 700 (2017) 198-208.
- [33] J.W. Cahn, The impurity-drag effect in grain boundary motion, *Acta Metall Mater* 10 (1962) 789-798.
- [34] R. Kainuma, Y. Fujita, H. Mitsui, I. Ohnuma, K. Ishida, Phase equilibria among α (hcp), β (bcc) and γ (L10) phases in Ti-Al base ternary alloys, *Intermetallics* 8 (2000) 855-867.
- [35] X.H. Wang, Y.C. Zhou, Layered Machinable and Electrically Conductive Ti_2AlC and Ti_3AlC_2 Ceramics: a Review, *J. Mater. Sci. Technol.* 26 (2010) 385-416.
- [36] P. Bartolotta, J. Barrett, T. Kelly, R. Smashey, The use of cast Ti-48Al-2Cr-2Nb in jet engines, *JOM* 49 (1997) 48-50.
- [37] L. Xiao, W. Lu, J. Qin, Y. Chen, D. Zhang, M. Wang, F. Zhu, B. Ji, Creep behaviors and stress regions of hybrid reinforced high temperature titanium matrix composite, *Compos Sci Technol* 69 (2009) 1925-1931.
- [38] X. Song, H. Cui, Y. Han, N. Hou, N. Wei, L. Ding, Q. Song, Effect of carbon reactant on microstructures and mechanical properties of TiAl/ Ti_2AlC composites, *Mat. Sci. Eng. A* 684 (2017) 406-412.

- [39] B.G. Liu, L.H. Liu, W.D. Xing, R.C. Liu, R. Yang, P.A. Withey, J. Zhu, R. Yu, Structural stability and the alloying effect of TiB polymorphs in TiAl alloys, *Intermetallics* 90 (2017) 97-102.
- [40] Q. Wang, H. Ding, H. Zhang, R. Chen, J. Guo, H. Fu, Influence of Mn addition on the microstructure and mechanical properties of a directionally solidified γ -TiAl alloy, *Materials Characterization* 137 (2018) 133-141.
- [41] Z. Wu, R. Hu, T. Zhang, H. Zhou, H. Kou, J. Li, Microstructure determined fracture behavior of a high Nb containing TiAl alloy, *Mat. Sci. Eng. A* 666 (2016) 297-304.
- [42] M. Schloffer, F. Iqbal, H. Gabrisch, E. Schwaighofer, F.-P. Schimansky, S. Mayer, A. Stark, T. Lippmann, M. Göken, F. Pyczak, H. Clemens, Microstructure development and hardness of a powder metallurgical multi phase γ -TiAl based alloy, *Intermetallics* 22 (2012) 231-240.

Accepted manuscript